J|A|C|S
ARTICLES
Published on Web 08/17/2002

Acetate Binding at the Photosystem II Oxygen Evolving Complex: An S_2-State Multiline Signal ESEEM Study

Keri L. Clemens, Dee Ann Force†, and R. David Britt*

Contribution from the Department of Chemistry, University of California, Davis, California 95616-0935

Received August 23, 2001. Revised Manuscript Received April 29, 2002

Abstract: Previously, using acetate deuterated in the methyl hydrogen positions, we showed that acetate binds in close proximity to the Mn cluster/$Y_Z^{\bullet}$ tyrosine dual spin complex in acetate-inhibited photosystem II (PSII) preparations exhibiting the "split" EPR signal arising from the $S_2-Y_Z^{\bullet}$ interaction [Force, D. A.; Randall, D. W.; Britt, R. D. *Biochemistry* **1997**, *36*, 12062−12070]. By using paramagnetic NO to quench the paramagnetism of $Y_Z^{\bullet}$, we are able to observe the ESEEM spectrum of deuterated acetate interacting with only the Mn cluster. A good fit of the ESEEM data indicates two ^{2}H dipolar hyperfine couplings of 0.097 MHz and one of 0.190 MHz. Modeling of these dipolar interactions, using our "dangler" 3 + 1 model for the S_2-state of the Mn cluster, reveals distances consistent with direct ligation of acetate to the Mn cluster. As acetate inhibition is competitive with the essential cofactor Cl^-, this suggests that Cl^- ligates directly to the Mn cluster. The effect of acetate binding on the structure of the Mn cluster is investigated by comparing the Mn-histidine coupling in NO/acetate-treated PSII and untreated PSII using ESEEM. We find that the addition of acetate and NO does not affect the histidine ligation to the Mn cluster. We also investigate the ability of acetate to access $Y_Z^{\bullet}$ in Mn-depleted PSII, a PSII preparation expected to be more solvent accessible than intact PSII. We detect no coupling between $Y_Z^{\bullet}$ and acetate. We have previously shown that small alcohols such as methanol can ligate to the Mn cluster with ease, while larger alcohols such as 2-propanol, as well as DMSO, are excluded [Force, D. A.; Randall, D. W.; Lorigan, G. A.; Clemens, K. L.; Britt, R. D. *J. Am. Chem. Soc.* **1998**, *120*, 13321−13333]. We probe the effect of acetate binding on the ability of methanol and DMSO to bind to the Mn cluster. We find that methanol is able to bind to the Mn cluster in the presence of acetate. We detect no DMSO binding in the presence of acetate. Thus, acetate binding does not increase the affinity or accessibility for DMSO binding at the Mn cluster. We also explore the possibility that the acetate binding site is also a binding site for substrate water. By comparing the ratioed three-pulse ESEEM spectra of a control, untreated PSII sample in 50% D_2O to an NO/acetate-treated PSII sample in 50% D_2O, we find that the binding of acetate to the oxygen evolving complex of photosystem II displaces deuterons bound very closely to the Mn cluster.

The oxidation of water to dioxygen is a light-driven process that occurs in the oxygen evolving complex (OEC) of photosystem II (PSII).[1−3] The redox-active cofactors are associated primarily with two major PSII membrane-spanning proteins, D1 and D2. A 33 kDa lumenally associated extrinsic protein, often termed the manganese stabilizing protein (MSP), is present in PSII reaction centers of higher plants and cyanobacteria, whereas two additional lumenally associated proteins of 23 and 17 kDa apparent molecular weight are found only in higher plant PSII centers. A tetranuclear manganese cluster is a core component of the OEC, along with a special redox-active tyrosine, Y_Z, and essential inorganic cofactors, Ca^{2+} and Cl^-. Water oxidation occurs via a cycle of five "S-states", S_{0-4},[4] where the manganese cluster is most reduced in the lowest S-state, S_0. Photooxidation of the Chl species P_{680} drives the S-state advancement through sequential oxidation of Y_Z and the Mn cluster (or of adjacent redox-active components of the OEC). Oxygen is released within a millisecond of the formation of the final state, S_4.

PSII membranes depleted of chloride do not evolve oxygen.[5−7] In addition, they do not exhibit the characteristic $g = 2$ S_2-state Mn multiline EPR signal upon illumination at 200 K.[8] XANES studies have suggested that the manganese cluster is advanced to the S_2-state in the absence of Cl^-, but there is some alteration in the magnetic environment of the cluster such that the S_2 multiline is not observed.[9] However, the S_2 multiline

* To whom correspondence should be addressed. E-mail: rdbritt@ucdavis.edu.
† Current address: Fresno County Public Health Laboratory, 1221 Fulton Mall, Fresno, CA 93721.

(1) Britt, R. D. In *Oxygenic Photosynthesis: The Light Reactions*; Ort, D. R., Yocum, C. F., Eds.; Kluwer Academic: Dordrecht, The Netherlands, 1996; pp 137−164.
(2) Debus, R. J. *Biochim. Biophys. Acta* **1992**, *1102*, 269−352.
(3) Yachandra, V. K.; Sauer, K.; Klein, M. P. *Chem. Rev.* **1996**, *96*, 2927−2950.
(4) Kok, B.; Forbush, B.; McGloin, M. *Photochem. Photobiol.* **1970**, *11*, 457−475.
(5) Coleman, W. J. *Photosynth. Res.* **1990**, *23*, 1−27.
(6) Homann, P. H. *J. Bioenerg. Biomembr.* **1987**, *19*, 105−121.
(7) Yocum, C. F. In *Manganese Redox Enzymes*; Pecoraro, V. L., Ed.; VCH: New York, 1992; pp 71−83.
(8) Ono, T.; Zimmermann, J.-L.; Inoue, Y.; Rutherford, A. W. *Biochim. Biophys. Acta* **1986**, *851*, 193−201.

EPR signal can be regenerated in chloride-depleted PSII preparations by the addition of Cl^- following flash-induced advancement to the S_2-state.[8]

While Cl^- is necessary for oxygen evolution, it can be replaced rather efficiently with Br^-, resulting in high levels of activity.[10] Oxygen evolution can be reactivated to a lesser extent by other ions such as NO_3^-, I^-, and OH^-.[10,11] However, exchanging chloride for F^-, amines, or acetate clearly inhibits oxygen evolution.[10,12,13] Sandusky and Yocum studied amine inhibition effects, including the relation to chloride binding.[12] All amines examined were found to bind at a site competitive with chloride.[12,14] Ammonia alone was also found to bind at a separate, chloride-independent site.[12,14] This second ammonia binding site was investigated with EPR spectroscopy, which demonstrated an alteration in the multiline EPR signal line shape upon ammonia binding;[15] later, ammonia was definitively shown to bind as a ligand to the Mn cluster using ESEEM (electron spin−echo envelope modulation).[16]

Sandusky and Yocum also demonstrated that the binding affinity for the chloride-competitive site increases with the basicity of the amines.[12,14] Other experiments have demonstrated that the binding affinity of chloride changes with the oxidation state of the Mn cluster, at least in the lowest S-states.[17] Both of these observations provide support to the possibility of direct chloride ligation to the manganese cluster.[12,14,17] In turn, direct ligation of Cl^- to the Mn cluster in one or more S-states provides a basis for a mechanistic role for Cl^- in the water oxidation process, in addition to any possible structural role. Indeed, recent experiments by Wincencjusz et al.[18,19] have shown that chloride is required for the $S_2 \rightarrow S_3$ and the $S_4 \rightarrow S_0$ transitions. Additionally, the kinetics of the $S_4 \rightarrow S_0$ transition were shown to be dependent on the type of anion occupying the Cl^- binding site, although no correlation was found between the pK_a, hardness/softness of the anions, etc. used in the study.[20] This dependence implies that the anion occupying the Cl^- site plays a role in the mechanism of water oxidation. A relevant example is the initial detailed hydrogen atom abstraction model for water splitting proposed by Babcock and co-workers.[21] In this model, $Y_Z^{\bullet}$ oxidizes an initial bound water via H-atom abstraction to the level of a terminal Mn═O species, while a Cl^- ligand bound at the second substrate binding site in the early S-states precludes additional water oxidation which could lead to peroxide formation. The Cl^- is then displaced by water in the second site, allowing full oxidation of the second water and the ultimate formation of dioxygen. A more recent H-atom abstraction model incorporates functions for both calcium and chloride.[22] In this model, both water molecules are bound to the cluster at the S_0-state, and Cl^- is found ligated to Ca^{2+}.[22] Water oxidation occurs as in the earlier model, except that Cl^- migrates to a binding site directly on the terminal Mn═O species by the S_2-state.[22] This model implicates Cl^- as essential for both the $S_2 \rightarrow S_3$ and the $S_3 \rightarrow S_0$ transitions, which is consistent with the results reported by Wincencjusz et al.[18,19] Other researchers have also suggested models which include Cl^-. Both Brudvig[23] and Pecoraro[24] present models in which calcium, chloride, and the Mn cluster are connected through a network of hydrogen bonds. In these models, only one Mn atom is involved in the redox chemistry,[23,24] consistent with the theoretical calculation of Siegbahn and Crabtree.[25] In S_1, both Pecoraro and Brudvig show one H_2O bound to the redox-active Mn atom, while a hydroxide is positioned as a ligand to the nearby calcium.[23,24] S-state advancements occur until a terminal Mn(V)═O is formed at S_4.[23,24] Oxygen is then formed by nucleophilic attack on the Mn oxo ligand by the hydroxide ligand on calcium.[23,24] Pecoraro shows Cl^- as a terminal Mn ligand;[24] in the Brudvig model, Cl^- serves as a bridge between Mn and calcium, controlling the nucleophilicity of calcium as Mn oxidation increases.[23] Other schemes have been proposed in which chloride does not play an active role in oxygen formation. For example, Klein and co-workers[26] have suggested a model which utilizes the formation of an oxyl radical on one of the μ-oxo bridges at S_3. Oxygen would then form as an O−O bond between two oxo groups on one of the dimers or by reaction of the oxyl radical with a OH^- or H_2O either on Mn or nearby.[26] The latter possibility has also been suggested by Crabtree and Siegbahn.[25] Other investigators have suggested that Cl^- affects electron transfer within the cluster;[12,14,18,19] for example, Boussac and Rutherford have suggested that Cl^- is involved in the regulation of redox potential for the cluster.[27]

Despite the appeal of postulating direct Cl^- ligation to the Mn cluster, it has not been demonstrated directly with any structural methods. For example, EXAFS studies have yet to conclusively demonstrate chloride ligation to the manganese cluster.[2,28−30] Penner-Hahn et al. note that to detect the coordination of a single chloride to the tetranuclear cluster, significant improvement in EXAFS signal-to-noise is necessary.[28] However, we note that Mn EXAFS data recorded on cyanobacteria in which Cl^- was replaced with Br^- were interpreted to favor a Br backscattering contribution corresponding to an Mn−Br distance of ∼2.5 Å.[31] It is also possible that the binding site for Cl^- is not on the cluster itself, but on a

(9) Ono, T.; Noguchi, T.; Inoue, Y.; Kusunoki, M.; Yamaguchi, H.; Oyanagi, H. *J. Am. Chem. Soc.* **1995**, *117*, 6386−6387.
(10) Kelley, P. M.; Izawa, S. *Biochim. Biophys. Acta* **1978**, *502*, 198−210.
(11) Damoder, R.; Klimov, V. V.; Dismukes, G. C. *Biochim. Biophys. Acta* **1986**, *848*, 378−391.
(12) Sandusky, P. O.; Yocum, C. F. *Biochim. Biophys. Acta* **1986**, *849*, 85−93.
(13) Sinclair, J. *Biochim. Biophys. Acta* **1984**, *764*, 247−252.
(14) Sandusky, P. O.; Yocum, C. F. *Biochim. Biophys. Acta* **1984**, *766*, 601−611.
(15) Beck, W. F.; Brudvig, G. W. *Biochemistry* **1986**, *25*, 6479−6486.
(16) Britt, R. D.; Zimmerman, J.-L.; Sauer, K.; Klein, M. P. *J. Am. Chem. Soc.* **1989**, *111*, 3522−3532.
(17) Wincencjusz, H.; Yocum, C. F.; van Gorkom, H. J. *Biochemistry* **1998**, *37*, 8595−8604.
(18) Wincencjusz, H.; van Gorkom, H. J.; Yocum, C. F. *Biochemistry* **1997**, *36*, 3663−3670.
(19) Wincencjusz, H. Ph.D. Dissertation; Biophysics Department, Huygens Laboratory, State University, The Netherlands, 1998.
(20) Wincencjusz, H.; Yocum, C. F.; van Gorkom, H. J. *Biochemistry* **1999**, *38*, 3719−3725.
(21) Hoganson, C. W.; Lydakis-Simantiris, N.; Tang, X.-S.; Tommos, C.; Warncke, K.; Babcock, G. T.; Diner, B. A.; McCracken, J.; Styring, S. *Photosynth. Res.* **1995**, *46*, 177−184.
(22) Tommos, C.; Babcock, G. T. *Acc. Chem. Res.* **1998**, *31*, 18−25.
(23) Limburg, J.; Szalai, V. A.; Brudvig, G. W. *J. Chem. Soc., Dalton Trans. (1972−1999)* **1999**, 1353−1361.
(24) Pecoraro, V. L.; Baldwin, M. J.; Caudle, M. T.; Hsieh, W.; Law, N. A. *Pure Appl. Chem.* **1998**, *70*, 925−929.
(25) Siegbahn, P. E. M.; Crabtree, R. H. *J. Am. Chem. Soc.* **1999**, *121*, 117−127.
(26) Liang, W.; Roelofs, T. A.; Cinco, R. M.; Rompel, A.; Latimer, M. J.; Yu, W. O.; Sauer, K.; Klein, M. P.; Yachandra, V. K. *J. Am. Chem. Soc.* **2000**, *122*, 3399−3412.
(27) Boussac, A.; Rutherford, A. W. *J. Biol. Chem.* **1994**, *269*, 12462−12467.
(28) Penner-Hahn, J. E.; Fronko, R. M.; Pecoraro, V. L.; Yocum, C. F.; Betts, S. D.; Bowlby, N. R. *J. Am. Chem. Soc.* **1990**, *112*, 2549−2557.
(29) Yachandra, V. K.; Guiles, R. D.; McDermott, A. E.; Cole, J. L.; Britt, R. D.; Dexheimer, S. L.; Sauer, K.; Klein, M. P. *Biochemistry* **1987**, *26*, 5974−5981.
(30) Yachandra, V. K.; DeRose, V. J.; Latimer, M. J.; Muderji, I.; Sauer, K.; Klein, M. P. *Science* **1993**, *260*, 675−679.
(31) Klein, M. P.; Sauer, K.; Yachandra, V. K. *Photosynth. Res.* **1993**, *38*, 265−277.

nearby amino acid.[32−35] Specifically, because the chloride requirement is correlated with pH, Homann proposed that the Cl^- site is located on a positively charged amino acid such as lysine or arginine, though it cannot be ruled out that this behavior could also arise from a metal binding site.[34]

Cl^--exchange studies using iodide have also been used to study the Cl^- binding site. Ikeuchi et al. found that Y_Z was subject to iodination when Cl^- was replaced by I^-.[36] Upon addition of Cl^-, iodination was prevented.[36] This would support Cl^- proximity to the cluster. In contrast, over the course of similar experiments, Rashid and Homann found iodide did not support specific iodination when very low concentrations of iodide were used.[37] Instead, iodination only seemed to occur when I^- was present in excess.[37] This is supported by recent investigations by Wincencjusz et al., using UV−vis to study the effects of chloride-exchange on electron transfer.[19] They found that the higher oxidation states of the OEC became subject to reduction by the replacement anion; reduction was shown to occur with I^- as well as NO_2^- and appeared to occur independent of the presence of Cl^-.[19] This supports the findings of Homann and Rashid in which I^- bound only at the Cl^- site and, when not present in excess, remains resistant to oxidation.[37] One might expect I^- to be vulnerable to oxidation if the binding site were located on the metal. Rashid and Homann proposed that the Cl^- site must be sequestered within a hydrophobic pocket if the binding site involves direct Mn cluster ligation.[37] Nevertheless, recent ^2H ESEEM experiments probing the results of ^2H_2O exchanged into the vicinity of the tyrosine radical $Y_Z^\bullet$, the Mn cluster, or the spin coupled Mn cluster/$Y_Z^\bullet$ dyad[38−41] show rapid contact with numerous water-derived deuterons. Thus, the environment of the OEC, including the surroundings of any Cl^- ligand to the cluster, does not appear to be hydrophobic. However, it is possible that the Cl^- site is as depicted in the more recent Babcock model,[21] in which case Cl^- is not actually bound directly to Mn until the S_2-state. This could explain the resistance of I^- to oxidation, at least in the earliest S-states. However, this possibility seems unlikely given the results of Wincencjusz et al. which determined that the binding affinity for chloride is much larger in S_1 than in S_2.[17] The lack of I^- oxidation at the Cl^- site could simply be due to a low redox potential of the coordinating Mn atom at that particular S-state.

On the analytical forefront, Lindberg et al. utilized radioactive ^{36}Cl to determine that there is one slowly exchangeable chloride per PSII reaction center.[42] They suggest the Cl^- binding site exists in two states, a native state with a strong binding constant and a state characterized by a weak binding constant.[43] The shift between the two states may be caused by the removal of the extrinsic proteins or by the higher pH used in the removal of the extrinsic proteins.[43] Lindberg et al. also found that the exchange of this Cl^- is not fully correlated with the loss of either oxygen evolution activity or the formation of the S_2-state multiline EPR signal.[42] This could indicate that, in fact, Cl^- is not intimately involved in the process of water oxidation or, alternatively, that it is not this particular chloride which is affecting oxygen evolution.[42] Another possibility is that the overall chloride depletion process, not the lack of chloride per se, introduces structural changes in the manganese cluster such that oxygen evolution is no longer possible without the readdition of Cl^-.[44]

As mentioned previously, acetate-treated PSII preparations do not evolve oxygen, although this inhibition can be alleviated by the addition of Cl^-.[12] Acetate-inhibited PSII preparations are blocked to advancement beyond the $S_2-Y_Z^\bullet$ state.[45] In chloride-depleted samples, this inhibition can be observed at low concentrations of acetate, similar to the Cl^- concentrations commonly used in PSII preparations.[10,46] Even in cases where both acetate and chloride are present at similar concentrations, the inhibition is still observed[12,46] and can be enhanced by increasing the concentration of acetate. Complete inhibition of oxygen evolution is achieved with high concentrations of acetate (200−600 mM).[47] For example, in the presence of 15 mM Cl^-, 660 mM acetate is needed for full inhibition; however, only 200 mM acetate is required when 1 mM Cl^- is present.[47] Typically, 400−500 mM acetate is used to prepare acetate-inhibited PSII preparations.[32,45,48] This high concentration of acetate is required because the binding affinity for acetate in the Cl^- site is much lower than it is for the native Cl^-.[46] Acetate-treated PSII quickly frozen following illumination at room temperature presents a characteristic "split" EPR signal centered at $g = 2$.[45,48] ^2H ESEEM of deuterated-tyrosine PSII particles,[49] ^{55}Mn ENDOR,[50] and EPR spectral simulations[50−52] have demonstrated conclusively that this "split" EPR signal arises from both the S_2-state of the Mn cluster and the trapped $Y_Z^\bullet$ radical interacting through a combination of exchange and dipolar couplings. Similar "split" interaction EPR spectra with somewhat varied line shapes are obtained by other PSII inhibition protocols, for example, depletion of the other essential inorganic cofactor, Ca^{2+}.[7,53,54]

We have previously used ESEEM of PSII membranes treated with methyl-deuterated acetate and illuminated to trap the "split" EPR signal to show that acetate binds in close proximity to the Mn−$Y_Z^\bullet$ dyad of PSII.[38] Because the special "split" signal line

(32) Coleman, W. J.; Govindjee. *Photosynth. Res.* **1987**, *13*, 199−223.
(33) Homann, P. H. *Biochim. Biophys. Acta* **1985**, *809*, 311−319.
(34) Homann, P. H. *Biochim. Biophys. Acta* **1988**, *934*, 1−13.
(35) Homann, P. H. *Plant Physiol.* **1988**, *88*, 194−199.
(36) Ikeuchi, M.; Koike, H.; Inoue, Y. *Biochim. Biophys. Acta* **1988**, *932*, 160−169.
(37) Rashid, A.; Homann, P. H. *Biochim. Biophys. Acta* **1992**, *1101*, 303−310.
(38) Force, D. A.; Randall, D. W.; Britt, R. D. *Biochemistry* **1997**, *36*, 12062−12070.
(39) Britt, R. D.; Peloquin, J. M.; Campbell, K. A. *Annu. Rev. Biophys. Biomol. Struct.* **2000**, *29*, 463−495.
(40) Diner, B. A.; Force, D. A.; Randall, D. W.; Britt, R. D. *Biochemistry* **1998**, *37*, 17931−17943.
(41) Tommos, C.; Tang, X.-S.; Warncke, K.; Hoganson, C. W.; Styring, S.; McCracken, J.; Diner, B. A.; Babcock, G. T. *J. Am. Chem. Soc.* **1995**, *117*, 10325−10335.
(42) Lindberg, K.; Vänngård, T.; Andréasson, L.-E. *Photosynth. Res.* **1993**, *38*, 401−408.
(43) Lindberg, K.; Andréasson, L.-E. *Biochemistry* **1996**, *35*, 14259−14267.
(44) Wydrzynski, T.; Baumgart, F.; MacMillan, R.; Renger, G. *Photosynth. Res.* **1990**, *25*, 59−72.
(45) Szalai, V. A.; Brudvig, G. W. *Biochemistry* **1996**, *35*, 1946−1953.
(46) Kühne, K. V.; Szalai, V. A.; Brudvig, G. W. *Biochemistry* **1999**, *38*, 6604−6613.
(47) Saygin, Ö.; Gerken, S.; Meyer, B.; Witt, H. T. *Photosynth. Res.* **1986**, *9*, 71−78.
(48) MacLachlan, D. J.; Nugent, J. H. A. *Biochemistry* **1993**, *32*, 9772−9780.
(49) Tang, X.-S.; Randall, D. W.; Force, D. A.; Diner, B. A.; Britt, R. D. *J. Am. Chem. Soc.* **1996**, *118*, 7638−7639.
(50) Peloquin, J. M.; Campbell, K. A.; Britt, R. D. *J. Am. Chem. Soc.* **1998**, *120*, 6840−6841.
(51) Dorlet, P.; Di Valentin, M.; Babcock, G. T.; McCracken, J. L. *J. Phys. Chem. B* **1998**, *102*, 8239−8247.
(52) Lakshmi, K. V.; Eaton, S. S.; Eaton, G. R.; Frank, H. A.; Brudvig, G. W. *J. Phys. Chem. B* **1998**, *102*, 8327−8335.
(53) Boussac, A.; Zimmermann, J.-L.; Rutherford, A. W. *Biochemistry* **1989**, *28*, 8984−8989.
(54) Hallahan, B. J.; Nugent, J. H. A.; Warden, J. T.; Evans, M. C. W. *Biochemistry* **1992**, *31*, 4562−4574.

shape originates from the electron spin coupling of $Y_Z^{\bullet}$ and the S_2-state of the Mn cluster, it is not trivial to determine if the observed modulation from nonexchangeable deuterons of the acetate methyl group results from a superhyperfine interaction with $Y_Z^{\bullet}$, with the Mn cluster, or with both spin centers. However, Szalai and Brudvig[55,56] have demonstrated that treatment of acetate-inhibited membranes with the paramagnetic NO molecule can quench the paramagnetism of the $Y_Z^{\bullet}$ radical. In this case, the "split" interaction spectrum is converted into the multiline EPR signal arising from the S_2-state of the Mn cluster alone. In this manuscript, we utilize this simplifying aspect of NO treatment, along with ESEEM targeting methyl-deuterated acetate, to test whether acetate binds in close proximity ($\leq$6 Å) of the Mn cluster in the S_2-state.

ESEEM permits the measurement of coupling between the unpaired electrons of the manganese cluster and nearby magnetic nuclei. One typically applies either two or three microwave pulses to produce electron spin−echoes. The microwave pulses induce both fully allowed ($\Delta M_S = \pm 1$; $\Delta M_I = 0$) and semi-allowed ($\Delta M_S = \pm 1$; $\Delta M_I \neq 0$) spin transitions;[57] consequently, the final wave function describing the system is a coherent superposition of states resulting from both the fully allowed and the semi-allowed spin transitions.[57,58] The interference in the time evolution of the components of the wave function creates a modulation of the spin−echo.[58] This modulation is directly dependent on the number, type, and distance of the nuclei from the electron spin. For example, we have previously investigated whether small alcohols could access the OEC using PSII samples treated with a series of ^{2}H-labeled alcohols.[59] In these samples, the only paramagnetic species probed in the "light minus dark" ESEEM time-domain difference spectrum is the S_2-state of the manganese cluster. As a result, one can use ESEEM to determine if the nonexchangeable deuterons of the alcohol are sufficiently close to the Mn cluster to give rise to modulation and, if so, to model Mn−^{2}H distances. As an intermediate step in the distance determination, we ratio the "light minus dark" time-domain ESEEM spectra obtained with deuterium-labeled alcohol-treated samples by the equivalent spectra from natural-abundance alcohol-treated preparations. This ratioing procedure suppresses ESEEM contributions from nuclei other than the acetate deuterons.[60] In addition, the modulation from proximal protons is experimentally suppressed by selecting a τ-value for the three-pulse experiment that is a multiple of the ^{1}H Larmor period.[58] Consequently, the data can be simulated as arising purely from the interaction between the net electron spin of the S_2-state manganese cluster and the nonexchangeable deuterons of the alcohol. We employ similar techniques in this paper.

Materials and Methods

Sample Preparation. PSII membranes were prepared from spinach on the basis of the procedure developed by Berthold, Babcock, and Yocum[61,62] with specific details provided by Campbell et al.[63] All steps were performed under dim green light or darkness in a coldroom. Isolated PSII membranes were resuspended in a buffer containing 400 mM sucrose, 20 mM MES−NaOH (pH 5.5, 6.0), 15 mM NaCl, 5 mM $MgCl_2$, and 5 mM $CaCl_2$, with subsequent storage in liquid nitrogen. All samples used for EPR spectroscopy were prepared at pH 5.5 or 6.0. Acetate-treated PSII membranes were prepared by washing PSII membranes twice in a buffer containing 400 mM sucrose and 40 mM MES−NaOH (pH 5.5, 6.0) (SM buffer). They were then washed once with a degassed buffer containing 400 mM sucrose, 40 mM MES−NaOH (pH 5.5, 6.0), and 400 mM sodium acetate (SMAc buffer), following the methods of Force et al.[38] and Szalai and Brudvig.[55] For all deuterated acetate-treated samples, the SMAc buffer was prepared with methyl-deuterated sodium acetate. Both the isotopically labeled and the natural-abundance SMAc buffers were adjusted to the correct pH using the corresponding isotopically labeled glacial acetic acid. D_2O-exchanged, acetate-treated PSII membranes were washed twice in SM buffer and then resuspended in a final wash buffer (SMAc pH 6.0) prepared with 50% D_2O. Samples treated with both acetate *and* deuterated methanol or deuterated DMSO were prepared similarly to acetate-only samples, except that the final wash buffer (SMAc pH 6.0) contained 1.0 M deuterated methanol or 1.0 M deuterated DMSO. Mn-depletion was based on the method of Tamura and Cheniae.[64] Mn-depleted/acetate-treated samples were prepared from PSII membranes by incubating in a buffer containing 400 mM sucrose, 40 mM MES−NaOH (pH 6.5), 15 mM NaCl, 1 mM EDTA, and 5 mM NH_4OH for 45 min in the dark. Samples were then washed twice in buffer containing 400 mM sucrose, 50 mM MES−NaOH (pH 6.0), and 1 mM EDTA (SME buffer) and, finally, in deuterated acetate SMAc buffer (pH 6.0). PSII samples were loaded into 3.8 mm o.d. precision quartz EPR tubes at a final chlorophyll concentration of 12−14 mg of Chl/mL (NO/acetate samples) or 13−18 mg of Chl/mL (untreated and acetate samples). PPBQ was added to a final concentration of 2 mM (from a 100 mM stock solution in DMSO). Samples were stored in liquid nitrogen until use.

Nitric oxide was added to the acetate-treated samples following the method of Szalai and Brudvig.[55] Samples in EPR tubes were degassed on a Schlenk line using two freeze−pump−thaw cycles; during the thaw cycle, the tube was kept in an ice/water slurry. The viscous sample would expand and coat the inner wall of the EPR tube for several centimeters by the final pump-thaw period. Following the introduction of 23−25 Torr of NO, the pressure was brought to 760 Torr with nitrogen. The final NO concentration was approximately 60−65-fold greater than the PSII concentration. The sample was quickly sealed, then spun down in an enclosed desktop centrifuge (2000 rpm) for 10 s, and frozen in liquid nitrogen. Alternatively, NO was added using a chemical donor (diethylamine NONOate; Cayman Chemical Co.). The donor was dissolved in a stock solution of degassed 0.01 M NaOH; once prepared, the solution can be stored on ice for up to 24 h. The weak NaOH solution used to suspend the NO donor had no apparent adverse effect on the sample; the addition of an aliquot of NaOH [equivalent to the donor suspension solution] to untreated PSII or acetate-treated PSII samples had no discernible effect on the EPR signals. Likewise, the base side product remaining after the release of NO from the donor demonstrated no adverse effects on the samples. Prior to donor addition, the sample-containing EPR tube was flushed with nitrogen; the NO donor concentration was approximately 700-fold greater than the PSII concentration. The sample was mixed, sealed, spun down, and frozen as stated above. We note that the NO donor procedure required a much larger apparent NO dose to quench $Y_Z^{\bullet}$ when compared to the pure gas procedure. This could in part be because of NO escape during the mixing period, when for a time the sample is

(55) Szalai, V. A.; Brudvig, G. W. *Biochemistry* **1996**, *35*, 15080−15087.
(56) Szalai, V. A.; Kühne, K. V.; Laksmi, K. V.; Brudvig, G. W. *Biochemistry* **1998**, *37*, 13594−13603.
(57) Kevan, L. In *Time-Resolved Electron Spin Resonance*; Kevan, L., Schwartz, R. N., Eds.; Wiley and Sons: New York, 1979; pp 280−341.
(58) Mims, W. B.; Peisach, J. In *Biological Magnetic Resonance*; Berliner, L. J., Ruben, J., Eds.; Plenum Press: New York, 1981; pp 213−263.
(59) Force, D. A.; Randall, D. W.; Lorigan, G. A.; Clemens, K. L.; Britt, R. D. *J. Am. Chem. Soc.* **1998**, *120*, 13321−13333.
(60) Mims, W. B.; Davis, J. L.; Peisach, J. *J. Magn. Reson.* **1990**, *86*, 273−292.
(61) Berthold, D. A.; Babcock, G. T.; Yocum, C. F. *FEBS Lett.* **1981**, *134*, 231−234.
(62) Ford, R. C.; Evans, M. C. W. *FEBS Lett.* **1983**, *160*, 159−164.
(63) Campbell, K. A.; Gregor, W.; Pham, D. P.; Peloquin, J. M.; Debus, R. J.; Britt, R. D. *Biochemistry* **1998**, *37*, 5039−5045.
(64) Tamura, N.; Cheniae, G. *Biochim. Biophys. Acta* **1987**, *890*, 179−194.

open to the atmosphere, in contrast to the gas procedure mixing step which is performed when the EPR tube is still attached to the Schlenk line. Acetate- and NO/acetate-treated samples were illuminated for 5 s at room temperature or 1 min on ice. It is noted that both illumination procedures produced ample "split" EPR signals and S_2 multiline EPR signals in the acetate- and NO/acetate-treated samples, respectively. However, the 1 min ice-temperature illumination procedure was favored to ensure diffusion of NO into the NO-treated samples. Untreated (pH 5.5, 6.0), methanol-only (pH 6.0), and DMSO-only (pH 6.0)-treated PSII samples were illuminated for 5 min at 200 K. To produce $Y_Z^\bullet$ and $Y_D^\bullet$ in the Mn-depleted/acetate-treated samples, the samples were positioned over a dry ice/methanol slurry (200 K), illuminated for 20 s, and then immersed in 200 K before removing the light source. The Mn-depleted/acetate-treated samples were subsequently warmed for 10 s on ice to eliminate $Y_Z^\bullet$ to observe only the $Y_D^\bullet$ radical species.

EPR Spectroscopy. CW-EPR spectra were collected at a temperature of 7 K using a Bruker ECS106 X-band CW-EPR spectrometer with an Oxford ESR900 liquid Helium cryostat and an ITC503 temperature controller. ESE field sweeps and ESEEM spectra were collected at a temperature of 4.2 K using a laboratory-built pulsed EPR spectrometer.[65] Two-pulse ESEEM experiments were performed by incrementing the time τ in the spin−echo sequence: $\pi/2 - \tau - \pi - \tau -$ echo. Three-pulse ESEEM experiments were performed by incrementing the time T in the stimulated echo sequence: $\pi/2 - \tau - \pi/2 - T - \pi/2 - \tau -$ stimulated echo. Time-domain ESEEM spectra were collected for both dark and illuminated samples; the "dark" spectra were subtracted from the "light" spectra to produce the "light minus dark" time-domain modulation patterns. A ratioing procedure was employed to simplify the three-pulse time-domain for samples treated with a deuterium-labeled molecule, such as deuterated acetate. The "light minus dark" modulation patterns, which were obtained for the deuterium-labeled and natural-abundance-treated PSII, were each normalized and then ratioed ($^2H/^1H$) to eliminate contributions to the ESEEM modulation from nuclei other than deuterons.[60] A cosine Fourier backfill was used to reconstruct the dead time data needed to generate the cosine Fourier transform.[66] ESEEM patterns were simulated using a FORTRAN program based on the density matrix formalism developed by Mims.[16,67,68]

Results

CW and Field-Swept ESE-EPR Spectra. Previous experiments by Szalai and Brudvig have demonstrated the reversible binding of NO to both $Y_D^\bullet$ and $Y_Z^\bullet$ in manganese-depleted PSII samples, as well as the paramagnetic-quenching of $Y_Z^\bullet$ by NO added to acetate-treated PSII, resulting in a "multiline" signal comparable to the control S_2-state signal.[55] By similar methods, we confirm the presence of NO bound to $Y_Z^\bullet$ in our NO/acetate-treated preparations. Figure 1 displays the "light minus dark" CW-EPR signals obtained for a series of three pH 5.5 PSII membrane samples. Figure 1a shows the "split" CW-EPR signal obtained from an acetate-treated PSII preparation without added NO. Addition of nitric oxide via the NO donor to an acetate-treated sample followed by ice-temperature illumination yields a multiline signal (1b), comparable to that displayed by the S_2-state of the Mn cluster in an untreated PSII sample (1c). The large "split" peaks resulting from the $S_2-Y_Z^\bullet$ interaction are completely quenched. We note that the EPR spectra of the NO/acetate-treated samples typically exhibit a large $g < 2$ NO signal due to the presence of excess NO. Thus, the mulitline signal on the high field side of the NO/acetate PSII spectrum is obscured and is not displayed in Figure 1b.

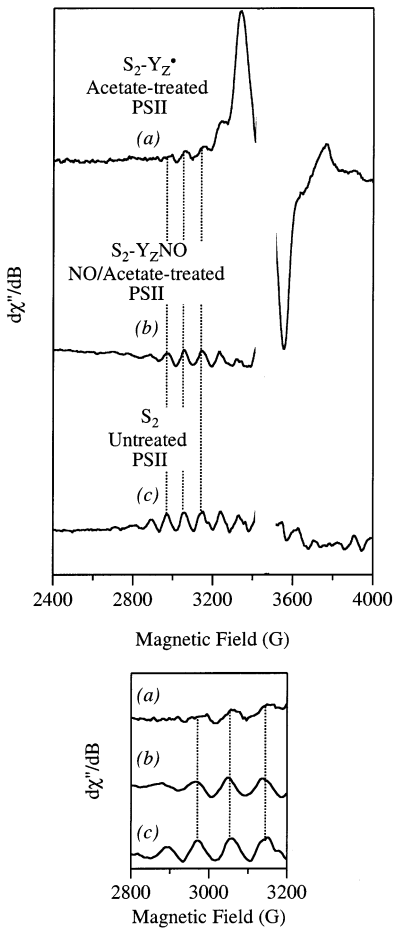

Figure 1. Derivative-mode CW-EPR spectra of (a) acetate-treated ($S_2-Y_Z^\bullet$), (b) NO/acetate-treated (S_2-Y_ZNO), and (c) untreated (S_2) PSII membranes pH 5.5 ("light minus dark" signals). Inset: expansion showing peak alignments. Spectra are offset for clarity. An NO donor (diethylamine NONOate) was used to release NO into the sample (see Materials and Methods for details). The dark spectra of all three samples were normalized to each other to account for any variation in concentration. The light spectra were then adjusted by the same factor used in the dark normalization, and the subtractions were performed. The high field side of the spectrum of the NO/acetate-treated sample is not shown due to the large NO signal. Experimental parameters: microwave frequency = 9.68 GHz; microwave power = 5 mW; modulation amplitude = 9.74 G; modulation frequency = 50 kHz; temperature = 7 K.

An expansion of Figure 1 (inset) more clearly displays the peak alignments. We observe that the resolved Mn hyperfine features on the low field side of the "split" signal in our acetate-treated PSII preparations (Figure 1, inset) are shifted from the Mn hyperfine peak positions of the control multiline signal. These shifts are significant (20 G) and reproducible, though smaller in magnitude than those reported by Szalai and Brudvig.[56] Moreover, the peaks of the multiline signal resulting from NO treatment of the acetate-inhibited samples (Figure 1b) line up well with the control multiline signal peaks, consistent with the interpretation that the shifts result from the $Y_Z^\bullet-$Mn cluster magnetic interactions,[50,52,56] which are quenched by the NO treatment. We are confident that we are performing both BBY preparation and acetate-inhibition procedures comparably to the Szalai and Brudvig experiments. Our BBY preparations exhibit O_2 evolution on par with that reported by Szalai and Brudvig.[55] In addition, we obtain amplitude ratios of the flanking multiline EPR features to the major "split" features in our acetate-treated samples that are comparable to those previously

(65) Sturgeon, B. E.; Britt, R. D. *Rev. Sci. Instrum.* **1992**, *63*, 2187−2192.
(66) Mims, W. B. *J. Magn. Reson.* **1984**, *59*, 291−306.
(67) Mims, W. B. In *Electron Paramagnetic Resonance*; Geschwind, S., Ed.; Plenum Press: New York, 1972; pp 263−351.
(68) Mims, W. B. *Phys. Rev. B* **1972**, *5*, 2409−2419.

reported.[56] As further verification that the acetate-treated samples are fully inhibited, we have found that 200 K illumination of acetate-treated PSII samples produces no S_2 multiline signal, whereas any uninhibited fraction would exhibit this multiline EPR signal under these illumination conditions. Therefore, our acetate-treated spectra do not appear to be contaminated by any significant contribution from untreated multiline signal.

We also note that over the course of these experiments, we have observed multiline signal amplitudes for the NO/acetate-treated samples as low as 40% of untreated PSII. The reduction in the signal amplitude is likely because of the interaction of NO with the dark S_1-state of the manganese cluster, denoted S_1-NO.[69] Goussias et al. found that ice-temperature incubation with NO on a time scale of minutes eliminated PSII advancement to S_2.[69] Some of our early experiments using the NO donor involved prolonged incubation of the samples on ice (10 min) to favor complete diffusion of NO into the sample; it is likely that some centers formed the S_1-NO state and were unable to advance further. This would lead to the observation of an undersized multiline signal in the NO/acetate-treated samples. Later experiments demonstrated that the incubation was unnecessary, and therefore we now minimize this effect by exposing the sample to ambient temperatures for as short of a time as possible during the process of NO addition. The fixed time required to add the NO to the sample using either method has limited us to obtaining S_2 multiline amplitudes that are typically 60−75% of the amplitudes of multiline EPR signals from control (untreated) samples.

To carry out the pulsed ESEEM experiments, it is important to characterize the field-swept electron spin−echo signals generated by illumination of our various PSII samples. Figure 2 displays the "light minus dark" ESE-EPR spectra (field values below $g = 2$) of acetate-treated PSII membranes (a), NO/acetate-treated membranes (b), and untreated membranes (c) (all pH 5.5). The ESE-EPR spectra reflect the direct EPR absorption line shape, rather than the field derivative, as no field modulation is employed. The acetate-treated sample shows a narrower ESE-EPR spectrum associated with a large contribution from the relatively narrow "split" portion of the interaction spectrum. This spectrum is comparable to those published in our previous ESE-ESEEM investigation of the acetate-inhibition form of the "split" signal.[38] The NO/acetate sample shows a broader ESE line width, essentially identical to that of the control multiline sample, with Mn hyperfine features evident in both spectra. There is no evidence of any free Mn(II) contamination in these spectra. We have found that long term (>10 min) exposure of the samples to NO, particularly at room temperature, releases some free Mn. This has also been observed by other researchers.[69,70] Indeed, long-term incubation of BBY membranes with mM concentrations of NO at −30 °C actually reduces the Mn cluster to a state below S_0.[69,71,72] The asterisks in Figure 2b mark the field positions (3100, 3180, and 3200 G) where the three-pulse ESEEM spectra were recorded for the NO/acetate-treated PSII preparations.

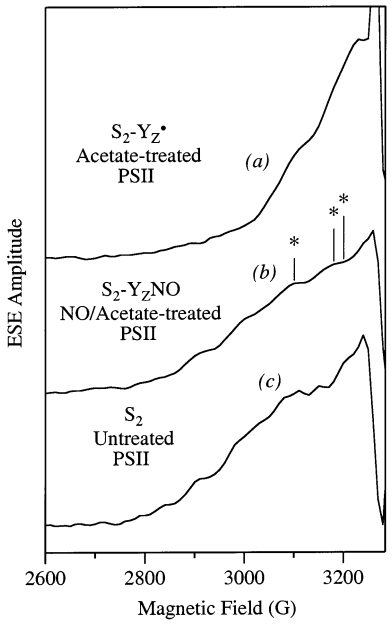

Figure 2. Absorption-mode ESE-EPR spectra of (a) acetate-treated ($S_2-Y_Z^\bullet$), (b) NO/acetate-treated (S_2-Y_ZNO), and (c) untreated (S_2) PSII membranes pH 5.5 ("light minus dark" signals). NO was added as in Figure 1. The spectra were normalized as in Figure 1 to account for concentration differences among the samples. Experimental parameters: microwave frequency = 9.184 GHz (untreated and NO/acetate-treated samples), 9.200 GHz (acetate-treated sample); microwave power = 32 W; repetition rate = 500 Hz; τ = 210 ns; $\pi/2$ pulse length = 15 ns; temperature = 4.2 K.

ESEEM. To test whether acetate ligation affects histidine ligation to the Mn cluster, we compared the histidine-Mn coupling of both NO/acetate-treated and untreated PSII using ESEEM.[73] Figure 3a shows the Fourier transforms of the two-pulse "light minus dark" time-domains for a series of four different NO/acetate-treated PSII samples (solid traces) in which NO was added as a gas; also shown is the Fourier transform of the two-pulse "light minus dark" time-domain of untreated (dotted trace) PSII membranes (pH 6.0). Figure 3b shows the average of the NO/CH_3COO^--treated samples as compared to the control sample. We observe no major changes in the modulation from the histidine ^{14}N nuclei, suggesting that the histidine ligation of the Mn cluster is unaffected by the addition of NO or acetate.

The three-pulsed time-domain ESEEM spectra (3200 G) of NO/acetate-treated samples (pH 5.5) in which NO was added as a gas are displayed in Figure 4. Included are the spectra for normal isotopic abundance acetate, deuterated (CD_3COO^-) acetate, and the $^2H/^1H$ ratio of these two spectra. The inset depicts the Fourier transform of the ratioed time-domain pattern; a single peak appears at the deuteron Larmor frequency (2.3 MHz). Similar results were obtained at 3100 and 3180 G (data not shown). Nitric oxide gas was also used to add NO to the samples for data collected at 3100 G, while the donor was used in the data set collected at 3180 G. Both methods of NO addition produce very similar time- and frequency-domain ESEEM spectra. The acetate deuteron modulation of the multiline signal electron spin−echo displayed here is appreciably deeper than our previously published acetate deuteron modulation of the $S_2-Y_Z^\bullet$ "split" signal.[38]

(69) Goussias, C.; Ioannidis, N.; Petrouleas, V. *Biochemistry* **1997**, *36*, 9261−9266.
(70) Sanakis, Y.; Goussias, C.; Mason, R. P.; Petrouleas, V. *Biochemistry* **1996**, *35*, 1411−1417.
(71) Sarrou, J.; Ioannidis, N.; Deligiannakis, Y.; Petrouleas, V. *Biochemistry* **1998**, *37*, 3581−3587.
(72) Ioannidis, N.; Sarrou, J.; Schansker, G.; Petrouleas, V. *Biochemistry* **1998**, *37*, 16445−16451.
(73) Tang, X.-S.; Diner, B. A.; Larsen, B. S.; Gilchrist, M. L.; Lorigan, G. A.; Britt, R. D. *Proc. Natl. Acad. Sci. U.S.A.* **1994**, *91*, 704−708.

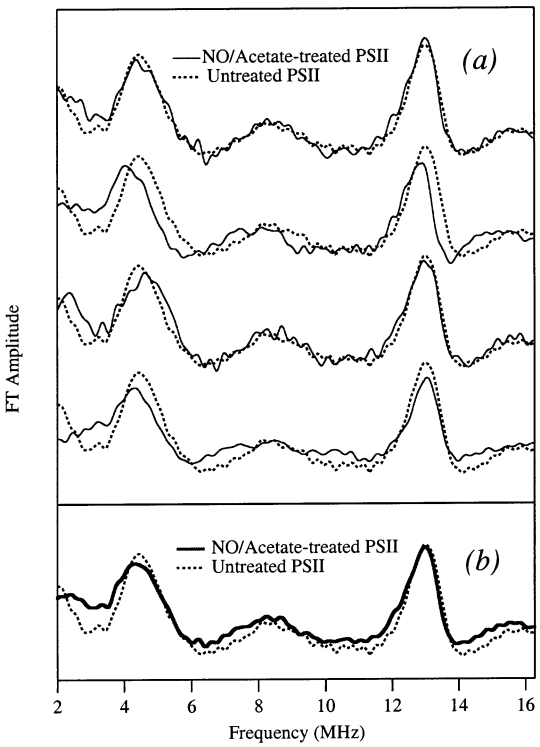

Figure 3. Fourier transforms of the "light minus dark" two-pulse ESEEM time-domain spectra obtained from: (a) a series of four different NO/acetate-treated (solid traces) PSII samples (pH 6.0) as compared to untreated (dotted trace) PSII membranes (pH 6.0); (b) the average of the four time-domain spectra for the NO/CH_3COO^--treated PSII samples (thick trace) as compared to the untreated (dotted trace) PSII control sample. Nitric oxide was added to the samples as a gas. Experimental parameters: microwave frequency = 9.234 GHz; B = 3100 G; starting τ = 170 ns; τ increment = 10 ns; microwave power = 25 W; repetition rate = 200 Hz; $\pi/2$ pulse length = 11 ns; π pulse length = 23 ns; temperature = 4.2 K.

Given the rapid dropoff of ^2H modulation depth with distance ($1/r^6$), this relatively strong ^2H modulation indicates that acetate, the only source of deuterons in the sample, is binding in very close proximity to the Mn cluster. For typical signal-to-noise levels, the maximum detectable distance for a weakly coupled deuteron is 5−6 Å. In our case, the peak is well above the noise level, suggesting a closer distance. An advantage of the relatively short range of ESEEM is that it discriminates against signals from low concentration solute molecules not bound at specific sites in close proximity to the metal center. For example, our earlier work on alcohol binding to the Mn cluster in the S_2-state revealed a K_d (at the temperature that the EPR sample formed a solid glass) of approximately 80 mM for methanol and ethanol.[59] At 80 mM concentration, approximately 0.005 nonspecifically bound alcohol molecules would occupy a hypothetical solvent-accessible cleft out to a distance of 6 Å, assuming a full octant of solvent accessibility (equivalent to a large solid angle of 1.6). Even at 400 mM, the concentration of acetate used for this study, only 0.03 nonspecifically bound acetate molecules would occupy such a cleft. A large number of more distant acetate molecules (R > 6 Å) cannot account for any appreciable contribution to the modulation, as the integrated modulation from such distant species drops off as R^{-4}. We therefore conclude that there is a specific acetate binding site in close proximity (<6 Å) to the Mn cluster.

Figure 5 addresses the issue of acetate access to the $Y_Z^\bullet$ center of Mn-depleted PSII preparations. The three-pulse

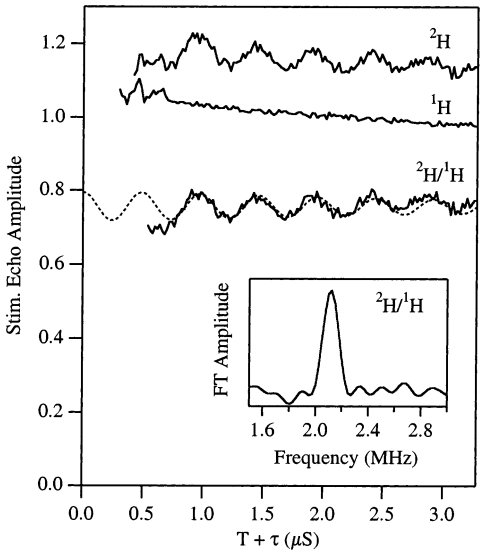

Figure 4. Time-domain "light minus dark" three-pulse ESEEM spectra of NO/CD_3COO^-, NO/CH_3COO^-, and $^2H/^1H$ ratioed NO/acetate-treated PSII membranes (pH 5.5). The Fourier transform of the $^2H/^1H$ ratioed time-domain is shown as an inset. Nitric oxide was added to the samples as a gas. The experimental data are shown as a solid line; a simulation is shown as a dotted line. Experimental parameters: microwave frequency = 9.168 GHz; B = 3200 G; τ = 220 ns; starting T = 80 ns; T increment = 20 ns; microwave power = 16 W; repetition rate = 200 Hz; $\pi/2$ pulse length = 15 ns; temperature = 4.2 K. Simulation parameters: $A_{iso} = 0$; $e^2Qq = 0.17$ MHz; electric field gradient asymmetry parameter $\eta = 0$; $A_{dip} = 0.097$, 0.190 MHz. See text for further simulation details.

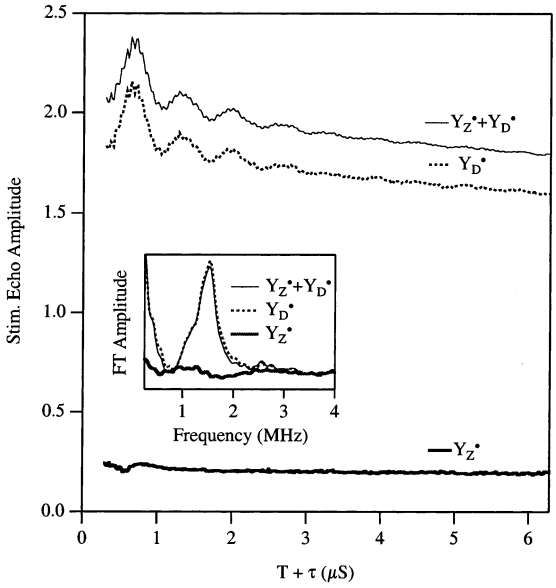

Figure 5. Time-domain and Fourier transform (inset) three-pulse ESEEM spectra of Mn-depleted/CD_3COO^--treated PSII membranes (pH 6.0): $Y_Z^\bullet$ trapped ($Y_D^\bullet$ and $Y_Z^\bullet$; "light"), $Y_D^\bullet$ only ("dark"), $Y_Z^\bullet$ only ("light minus dark"). Experimental parameters: microwave frequency = 9.234 GHz; B = 3100 G; τ = 214 ns; starting T = 86 ns; T increment = 20 ns; microwave power = 25 W; repetition rate = 200 Hz; $\pi/2$ pulse length = 11 ns; temperature = 4.2 K.

ESEEM modulation pattern for $Y_Z^\bullet$ alone (Figure 5, lowest trace) is isolated from the trace of the "illuminated" $Y_Z^\bullet$ + $Y_D^\bullet$-trapped CD_3COO^--treated/Mn-depleted PSII sample (upper trace) by subtracting the "dark" spectrum of the annealed sample (middle trace), which contains only $Y_D^\bullet$. The inset depicts the corresponding Fourier transforms of the three-pulse

ESEEM spectra. The low-frequency modulation, corresponding to the ~1.5 MHz peak in the Fourier transforms, arises from a β methylene proton of the $Y_D^\bullet$ radical which is close to the "exact cancellation" condition which gives rise to large ESEEM intensities.[74,75] However, we observe no ^2H modulation which would result from deuterated acetate binding in the vicinity of $Y_Z^\bullet$ in the Mn-depleted sample. Given that $Y_Z^\bullet$ in Mn-depleted PSII particles is thought to be more solvent accessible than in Mn-intact PSII particles,[40,76,77] this reinforces the argument made above that one is unlikely to see nonspecific binding at the 400 mM concentration of the deuterated acetate used here. Moreover, given our previous result that ^2H modulation is observed from deuterated acetate bound in the vicinity of the Mn cluster/$Y_Z^\bullet$ dyad of PSII giving rise to the "split" EPR signal,[38] this new experiment showing an abolition of this modulation as seen from the $Y_Z^\bullet$ species when the Mn cluster is destroyed suggests a role of the intact Mn cluster in establishing this acetate binding site.

We have previously used ESEEM to show that in intact BBY membranes, small alcohols such as methanol bind at the Mn cluster, while bulkier alcohols such as 2-propanol, as well as DMSO, are unable to access the cluster.[59] Given that ^2H ESEEM provides a powerful probe to investigate the binding of deuterated alcohols and DMSO as described above, we have performed an initial set of experiments using 1.0 M deuterated methanol (which binds in a control, non-acetate-treated sample) and 1.0 M deuterated DMSO (which does not) to examine the effect of acetate binding on the access of these potential ligands to the Mn cluster. NO was added to these samples as a gas. Sample treatment details are provided in the Materials and Methods section. We first determined that we can produce reasonable multiline EPR signals in PSII samples treated with NO/CH_3COO^-/d_4-methanol and NO/CH_3COO^-/d_6-DMSO. These samples produce multiline signals that are similar to those exhibited by NO/acetate-treated samples. Figure 6a displays the Fourier transform of the three-pulse ESEEM time-domain of a control PSII sample (pH 6.0) treated with deuterated methanol only (thick trace) and a set of Fourier transforms corresponding to four different PSII preparations (pH 6.0) treated with NO/CH_3COO^-/d_4-methanol (thin traces). We performed the ESEEM experiment with multiple samples to check for consistency. We note that there is some variance from sample to sample, but all show appreciable ^2H modulation from deuterated methanol bound in close proximity to the Mn cluster in the presence of acetate. Figure 6b shows the average (dotted trace) of the NO/CH_3COO^-/d_4-methanol-treated samples as compared to the control sample. We observe that the deuteron modulation in the acetate-treated samples is quite comparable to that of the control. This indicates that acetate binding does not eliminate methanol binding in close proximity to the Mn cluster.

Figure 7a presents the Fourier transform of the three-pulse time-domain of a control PSII sample (pH 6.0) treated with deuterated-DMSO (thick trace) and the Fourier transforms of three different PSII samples (pH 6.0) each treated with NO/CH_3COO^-/d_6-DMSO (thin traces). Figure 7b compares the average of these three data sets (dotted trace) to the control. We see that as for the non-acetate-treated control, there is no evidence for DMSO binding near the Mn cluster.[59] DMSO does not bind to the Mn cluster in a control sample, either because it is too bulky to access the site occupied by methanol or perhaps because its intrinsic binding affinity is significantly lower than that of methanol. Acetate binding at the Mn cluster does not open a new proximal DMSO binding site. This is not a surprising result. However, the lack of appreciable ^2H modulation from d_6-DMSO at 1.0 M concentration experimentally reinforces the point that these ESEEM experiments effectively discriminate against detection of molecules dispersed in solvent distributed over multiple nonspecific binding sites. The deuterated DMSO concentration used here is 2.5 times greater than that of the deuterated acetate used in Figure 4, and the ^2H concentration provided is greater by a factor of 5.

We can also explore water binding to the Mn cluster using ^2H ESEEM following D_2O incubation.[1,39] Figure 8a compares the three-pulse ratioed (50% D_2O/H_2O) time-domain spectra and Fourier transforms (inset) for sets of three control and four NO/

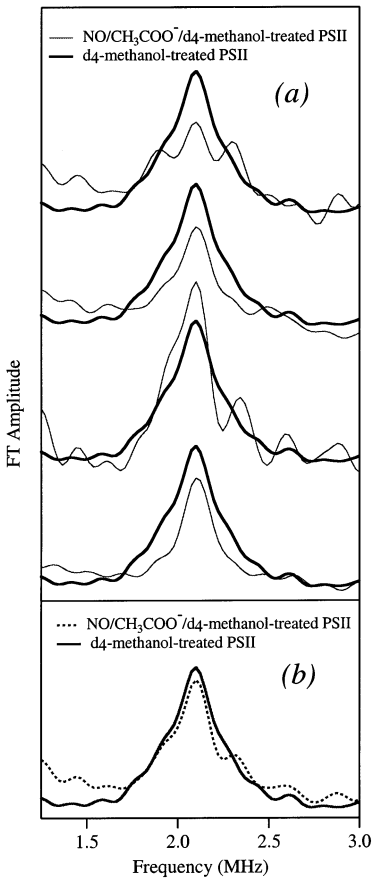

Figure 6. Fourier transforms of the "light minus dark" three-pulse ESEEM time-domain spectra obtained from: (a) a series of four different PSII samples treated with NO/CH_3COO^-/d_4-methanol (thin traces) as compared to PSII membranes (pH 6.0) treated with d_4-methanol only (thick trace); (b) the average of the four time-domain spectra for the NO/CH_3COO^-/d_4-methanol-treated samples (dotted trace) as compared to that of the d_4-methanol (thick trace) PSII control sample. Nitric oxide was added to the samples as a gas. See Materials and Methods for sample treatment details. Experimental parameters: microwave frequency = 9.405 GHz; B = 3200 G; τ = 220 ns; starting T = 80 ns; T increment = 20 ns; microwave power = 16 W; repetition rate = 200 Hz; $\pi/2$ pulse length = 11 ns; temperature = 4.2 K.

(74) Evelo, R. G.; Hoff, A. J.; Dikanov, S. A. *Chem. Phys. Lett.* **1989**, *161*, 479−484.
(75) Warncke, K.; McCracken, J. *J. Chem. Phys.* **1994**, *101*, 1832−1841.
(76) Babcock, G. T.; Espe, M.; Hoganson, C.; Lydakis-Simantiris, N.; McCracken, J.; Shi, W.; Styring, S.; Tommos, C.; Warncke, K. *Acta Chem. Scand.* **1997**, *51*, 533−540.
(77) Tommos, C.; McCracken, J.; Styring, S.; Babcock, G. T. *J. Am. Chem. Soc.* **1998**, *120*, 10441−10452.

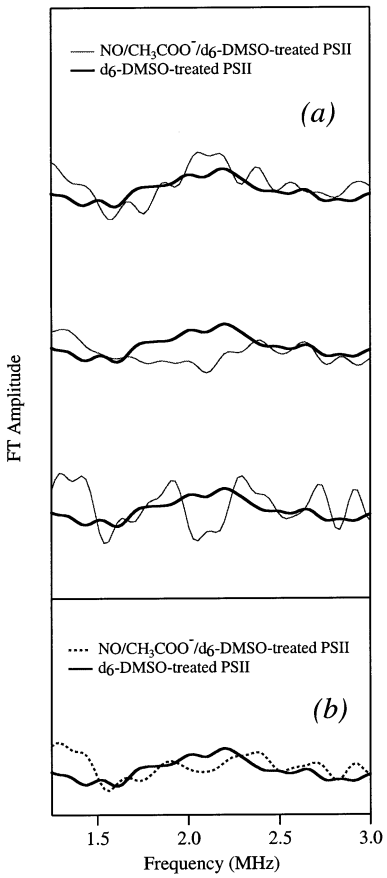

Figure 7. Fourier transforms of the "light minus dark" three-pulse ESEEM time-domain spectra obtained from: (a) a series of three different PSII samples treated with NO/CH_3COO^-/d_6-DMSO (thin traces) as compared to PSII membranes (pH 6.0) treated with d_6-DMSO only (thick trace); (b) the average of the three time-domain spectra for the NO/CH_3COO^-/d_6-DMSO-treated samples (dotted trace) as compared to that of the d_6-DMSO (thick trace) PSII control sample. Nitric oxide was added to the samples as a gas. See Materials and Methods for sample treatment details. Experimental parameters are as in Figure 6.

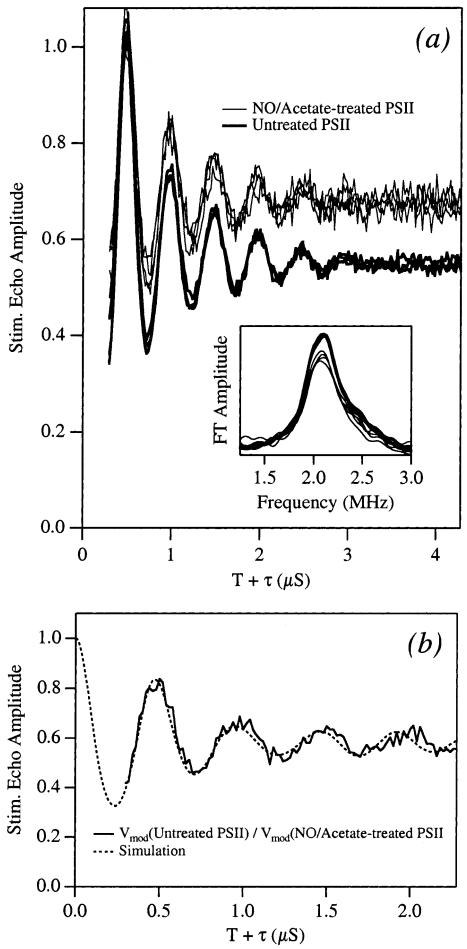

Figure 8. (a) Time-domain "light minus dark" three-pulse ESEEM spectra of ratioed (50% D_2O/H_2O) NO/CH_3COO^--treated (thin traces; four separate sample sets) and (50% D_2O/H_2O) untreated (thick traces; three separate sample sets) PSII membranes (pH 6.0). Nitric oxide was added as a gas. The Fourier transforms of the ESEEM time-domain spectra are shown as an inset. (b) The three-pulse ESEEM time-domain "ratio of ratios" for a control PSII sample set and a NO/CH_3COO^--treated PSII sample set. The "ratio of ratios" is obtained by dividing a (50% D_2O/H_2O) ratioed "light minus dark" time-domain spectrum of untreated PSII by a (50% D_2O/H_2O) ratioed "light minus dark" time-domain spectrum of NO/CH_3COO^--treated PSII. The dotted trace corresponds to a simulation of the "ratio of ratios." Experimental parameters: microwave frequency = 9.234 GHz; B = 3100 G; τ = 227 ns; starting T = 73 ns; T increment = 20 ns; microwave power = 25 W; repetition rate = 200 Hz; $\pi/2$ pulse length = 11 ns; temperature = 4.2 K. Simulation parameters: $e^2Qq = 0.22$ MHz; electric field gradient asymmetry parameter $\eta = 0.1$; one deuteron ($A_{iso} = 0.800$ MHz; $A_{dip} = 0.617$ MHz) and two deuterons ($A_{dip} = 0.450$ MHz).

CH_3COO^--treated PSII membranes (samples prepared with 50% D_2O buffer were incubated 25 min; nitric oxide was added as a gas). We are currently using only 50% D_2O because the modulation from buffer prepared with 100% D_2O is so great we are concerned that small changes may be masked because of possible nonlinearities of the heavily modulated data sets. The ^2H modulation patterns are dramatically different between the two classes of samples, with reduced modulation found in the acetate inhibited samples relative to the uninhibited controls. This clearly indicates that acetate binding reduces the accessibility to the Mn cluster of deuterons of bound substrate waters or hydroxides, of other proximal waters, or of deuterons exchanged into other nearby sites.

Discussion

Histidine Nitrogen Ligation. In a previous ^{55}Mn ENDOR study of the "split" EPR signal,[50] we showed that the S_2-state ^{55}Mn hyperfine couplings of the tetranuclear Mn cluster are essentially unaltered by the introduction of the magnetic interaction with the $Y_Z^\bullet$ radical. This is consistent with the very similar line shapes of the multiline EPR signals for control [untreated] samples as compared to NO/acetate-treated samples, in which the $Y_Z^\bullet$ paramagnetism is quenched by the paramagnetic NO, revealing the multiline line shape rather than the "split" signal line shape (Figure 1).[45,55] With ESEEM, we can examine weaker hyperfine couplings to magnetic nuclei of ligands or other proximal molecules. ESEEM studies of control S_2-state samples show ^{14}N modulation patterns[73] that have been assigned to one or more histidine ligands via experiments using PSII particles prepared with ^{15}N labeled histidine.[73] Figure 3 shows that this ^{14}N-histidine modulation is very similar in the NO/acetate-treated sample when compared to a control S_2-state sample. This provides another demonstration that the electronic structure of the NO/acetate-treated sample is very similar to that of a control S_2-state sample. Furthermore, this demonstrates that acetate binding in the vicinity of the Mn cluster does not result in the removal of one or more histidine ligands.

Acetate Binding. Figure 4 shows that ^{2}H modulation of the multiline ESE signal results from the use of methyl-deuterated acetate in NO/acetate-treated PSII preparations. In the Results section, we argue that this modulation arises from deuterated acetate bound at a specific binding site in close proximity (<6 Å) to the Mn cluster. In this section, we address the range of possible distances between the Mn cluster and the acetate methyl deuterons which could give rise to the observed modulation. Such an estimate is needed to test whether acetate could be binding directly as a ligand to the cluster. There are several levels of analysis that can be used to estimate the actual Mn−^{2}H distance(s).[59] We start by magnetically modeling the Mn cluster as a point electron dipole. A straightforward analytical procedure[59,60,78] can then be used to estimate the electron−nuclear distance. As an initial estimate, we can quantify a range of distances between this electron point-dipole and the acetate methyl deuterons by using the "single nucleus/equivalent nuclei" approximations.[59,79] Implicit here is the assumption that a single acetate occupies the specific binding site probed by ESEEM, consistent with the data presented by Kühne et al. in which they proposed the existence of a single acetate binding site on the donor side of PSII.[46] The "single nucleus" approximation assumes that a single close methyl deuteron is the primary contributor to the signal modulation depth ($\bar{k}$) observed in the ESEEM time-domain. This approximation provides an approximate minimum distance, and, using the analytical procedure outlined in the footnote,[80] we can estimate this minimum distance between the electron point-dipole and the single acetate deuteron to be 3.7 Å ($\bar{k} = 0.084$). An upper approximation to the ^{2}H−Mn distance is derived using the "equivalent nuclei" approximation, which treats all three methyl deuterons as equidistant and therefore as equal contributors to the modulation. The equivalent nuclei approximation elicits a distance greater than the single nucleus approximation by a factor of $3^{1/6}$,[79] providing a maximal distance to the three equivalent methyl deuterons of 4.4 Å. Despite using one versus three deuterons in the two approximations, the 3.7−4.4 Å range is relatively tight due to the steep $1/r^6$ distance dependence.

A further-improved estimation of the ^{2}H−Mn distance can be obtained using a simulation method based on density matrix theory,[16,68] but still approximating the Mn cluster as a single point-dipole. Figure 4 shows a simulation of this type (dotted line) as an overlay to the experimental ratioed ESEEM data (solid line) obtained at 3200 G for NO/acetate-treated PSII membranes. Implicit to these simulations is a zero contact hyperfine interaction; thus, the electron nuclear spin hyperfine interaction is treated entirely as due to dipolar coupling. Accordingly, radial distances can be calculated from the simulated dipolar couplings using the equation

$$A_{\mathrm{dip}} = \frac{g\beta g_n \beta_n}{r^3} \tag{6}$$

where g, g_n, β, and β_n are the g-values and magnetons for the electron and nucleus, respectively. A quadrupolar coupling e^2Qq of 0.17 MHz is used for the $I = 1$ deuteron as measured for glycine ($NH_2CD_2COO^-$).[81] The quadrupole z-axis was approximated as collinear with the dipolar coupling axis, which is adequate for modeling the first few cycles of the ^{2}H modulation pattern. The simulation displayed in Figure 4 uses two deuterons with dipolar couplings of 0.097 MHz, corresponding to a 5.0 Å distance, and a single deuteron with a 0.190 MHz coupling, corresponding to a 4.0 Å distance.[82] Though we would not argue that this is a unique simulation, we clearly find boundaries as to what provides good simulations. For example, poorer simulations are obtained using a dipolar coupling which corresponds to a ^{2}H−Mn distance of $r < 3.0$ Å, or with all deuterons at $r > 5.0$ Å. Moreover, the simulation using two deuterons at 5.0 Å and one deuteron at 4.0 Å is better than simulations using one deuteron at 3.7 Å (from the analytical single nucleus approximation) or three deuterons at 4.4 Å (from the equivalent nuclei approximation). We therefore favor an intermediate coupling assignment, where all three deuterons contribute to the modulation, but not equally. This simulation is consistent with a single acetate site located in close proximity of the Mn cluster.

The next level of improvement in our analysis is to better model the Mn cluster. Instead of using a single point-dipole approximation, we can spatially distribute dipoles using a *multiple* point-dipole methodology which considers the center

(78) Lorigan, G. A.; Britt, R. D.; Kim, J. H.; Hille, R. *Biochim. Biophys. Acta* **1994**, *1185*, 284−294.
(79) Halkides, C. J.; Farrar, C. T.; Larsen, R. G.; Redfield, A. G.; Singel, D. J. *Biochemistry* **1994**, *33*, 4019−4035.

(80) For weak dipolar coupling between an $S = {}^1/_2$ electron and an $I = {}^1/_2$ nucleus, the theoretical modulation depth parameter (k) is given by:[60]

$$k_{I=1/2} = \left[\left(\frac{3g\beta}{H_o r^3}\right)\cos\theta\sin\theta\right]^2 \tag{1}$$

where g is equal to the g-value for the paramagnetic species, β represents the Bohr magneton, H_o is the magnitude of the applied magnetic field, r is the distance between the unpaired electron and the nuclei, and θ is the angle between the Zeeman field vector and the vector connecting the electron and the nucleus. The equation is simplified using the trigonometric identity $\cos\theta\sin\theta = {}^1/_2\sin 2\theta$:

$$k_{I=1/2} = \left[\left(\frac{3g\beta}{2H_o r^3}\right)^2\sin^2 2\theta\right] \tag{2}$$

For an $I = 1$ nucleus, such as ^{2}H, neglecting the effects of the small ^{2}H quadrupolar moment, the depth parameter will be ${}^8/_3$ times larger because k is proportional to $I(I+1)$:[60]

$$k_{I=1} = 6\left(\frac{g\beta}{H_o r^3}\right)^2\sin^2 2\theta \tag{3}$$

This equation is averaged over a sphere to account for the range of orientation of the magnetic field with respect to the vector between electron and nuclear spins:[60]

$$\bar{k}_{I=1} = \left(\frac{16}{5}\right)\left(\frac{g\beta}{H_o r^3}\right)^2 \tag{4}$$

The above equation can be used to calculate the distance between the nuclei and the unpaired electron spins, once a correction is made for the decay. A decay factor must be included to account for the damping of the modulation observed in the time domain: $\cos[0.378(m\pi/r^3)g\beta/H_o]$,[60,78] where m is dependent on the time ($T + \tau$). For example, m is equal to 3 for a ^{2}H cycle centered around the trough located $1{}^1/_2$ periods from ($T + \tau$) = 0; for the subsequent trough, m is equal to 5. By multiplying the modulation decay factor by the averaged theoretical modulation depth parameter, one obtains a corrected value for $\bar{k}$ that may be compared with the experimental data. The experimental modulation depth (d) can be determined using the following equation:[60,78]

$$d = \frac{-\frac{1}{2}[y(\mathrm{peakA}) + y(\mathrm{peakB})] - y(\mathrm{trough})}{-\frac{1}{2}[y(\mathrm{peakA}) + y(\mathrm{peakB})]} \tag{5}$$

where y represents the electron spin−echo amplitude at a particular time point ($T + \tau$).
(81) Edmonds, D. T. *Phys. Rep.* **1977**, *29*, 233−290.
(82) One consideration is whether the methyl group is frozen in a fixed orientation at the 4.2 K experimental temperature. The activation energy for methyl group rotation is 2.5 kcal/mol for CD_3COO^-, as determined by EPR experiments on irradiated crystalline acetic acid over the temperature range 77−130 K.[83] At 4.2 K, the amount of thermal kinetic energy available (kT) is merely 0.012 kcal/mol. Consequently, we consider the methyl group to be fixed at the low ESEEM observation temperature.

of each of the four manganese ions as a separate point-dipole.[59,84] In this case, each manganese contributes to the total dipolar coupling tensor. A_{dip} may be expressed as follows:[84]

$$A_{dip}^{total} = \sum_i \rho_i (A_{dip})_i \quad (7)$$

where ρ represents the spin projection factor that is dependent on the oxidation state of each manganese atom and the exchange coupling scheme employed. A_{dip} is numerically calculated over three-dimensional space about a given structural and magnetic model of the Mn cluster.[59,84] This procedure leads to three-dimensional isosurfaces of constant dipolar coupling strength.

For our three-dimensional modeling, we use our EPR/ENDOR-derived "dangler" model, with spin projection factors determined by ^{55}Mn ENDOR.[39,85] This model consists of a strongly antiferromagnetically coupled trinuclear core, with an adjacent, more weakly coupled fourth Mn. Figure 9 shows planar slices through the contours of constant dipolar hyperfine coupling $A_{dip} = 0.097$ and 0.190 MHz, the same values which we used to simulate the ESEEM spectra (see Figure 4). Superimposed over the planar slices are possible acetate binding motifs (described below). For discussion, from left to right, the Mn atoms are denoted Mn(a−d). In the model presented in Figure 9, Mn(b) has an oxidation state of +3, while Mn(a,c,d) all have +4 oxidation states. The spin projection factors are as follows: Mn(a), $\rho = -0.90$; Mn(b), $\rho = 1.62$; Mn(c), $\rho = -0.95$; Mn(d), $\rho = 1.22$.[85] Utilizing these contour plots, we can extract a range of possible distances from the deuterium nuclei to nearest Mn ion of the cluster. We find a range of 3.9−6.1 Å corresponding to the weakest dipolar coupling, $A_{dip} = 0.097$ MHz; for the stronger coupling, $A_{dip} = 0.190$ MHz, we obtain a span of 3.5−5.6 Å.

These ESEEM simulations generate acetate−Mn distances which are consistent with direct acetate ligation. As mentioned previously, Figure 9 displays three possible geometries of the acetate-treated manganese cluster, superimposed over planar slices of constant dipolar hyperfine $A_{dip} = 0.097$ and 0.190 MHz for the "dangler" model of the tetranuclear Mn cluster.[85] Acetate could ligate directly to the cluster in several ways. Figure 9a shows acetate bound to the Mn cluster through a monodentate linkage at three different Mn positions. As before, the Mn atoms are designated Mn(a−d), from left to right. Although not shown in Figure 9a, monodentate binding is possible from Mn(b) as well. Figure 9b shows a bidentate linkage from Mn(a). This type of binding motif could also occur from Mn(c). Analogous binding from the other two Mn positions is not supported within the context of this model. Finally, Figure 9c shows a carboxylato bridge between Mn(c) and Mn(d). A bridge initiating from either Mn(a) or Mn(b) is not supported by this model. In summary, our analysis of the ESEEM data demonstrates that these experimental results are consistent with direct ligation of acetate to the Mn cluster, either as a simple monodentate ligand, as a bidentate ligand, or as a bridge between two Mn ions of the cluster. In addition, we cannot rule out the possibility that acetate ligates to a nearby amino acid in such a way that the acetate deuterons are positioned in very close proximity to the cluster.

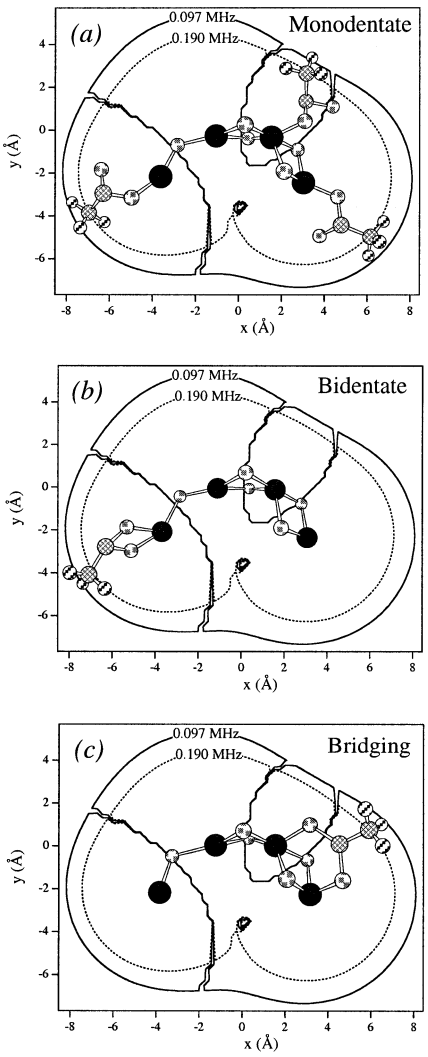

Figure 9. Three possible models for the acetate-treated manganese cluster, superimposed on a slice through the $A_{dip} = 0.190$ MHz (dotted line) and 0.097 MHz (solid line) ^{2}H hyperfine isosurfaces using the "dangler" model. The "seams" though the center of the contours correspond to nodal areas. For discussion, the Mn atoms are denoted Mn(a−d), from left to right, which corresponds to a Mn(IV,III,IV,IV) valence assignment. The spin projection factors are as follows: Mn(a): $\rho = -0.90$; Mn(b): $\rho = 1.62$; Mn(c): $\rho = -0.95$; and Mn(d): $\rho = 1.22$.[85] Three possible motifs for the acetate binding site are shown: monodentate (a), bidentate (b), and bridging ligation (c). Panel a shows the monodentate ligation of acetate to any one of three possible sites (only a single acetate is thought to be bound). We show the monodentate ligation of acetate to Mn(a), Mn(c), and Mn(d), although ligation to Mn(b) is not entirely unlikely. Panel b depicts bidentate linkage to Mn(a); this type of linkage could also occur to Mn(c). Panel c shows the lone possibility of a bridge between two Mn atoms, Mn(c,d). Model key: Mn (black); O (dotted); C (narrow stripes); D (wide stripes).

Enzyme kinetic plots have demonstrated binding competition between Cl^- and amines, as well as between Cl^- and F^-.[12,14] It is also well established that acetate and F^- inhibit oxygen evolution and that this inhibition can be mitigated by Cl^-.[12] Because acetate behaves in a manner similar to F^- with regard to effect on oxygen evolution, and also acts as a Lewis base, as do amines, it seems reasonable to expect that acetate would also be competitive with Cl^-. Brudvig and co-workers[46] have recently performed an extensive study of the relationship between acetate and chloride using kinetic analysis and EPR

(83) Erickson, R.; Nordh, U.; Benetis, N. P.; Lund, A. *Chem. Phys.* **1992**, *168*, 91−98.
(84) Randall, D. W.; Gelasco, A.; Caudle, M. T.; Pecoraro, V. L.; Britt, R. D. *J. Am. Chem. Soc.* **1997**, *119*, 4481−4491.
(85) Peloquin, J. M.; Campbell, K. A.; Randall, D. W.; Evanchik, M. A.; Pecoraro, V. L.; Armstrong, W. H.; Britt, R. D. *J. Am. Chem. Soc.* **2000**, *122*, 10926−10942.

measurements. From kinetic studies of steady-state oxygen evolution rates at different concentrations of both acetate and Cl^-, these investigators found that acetate binds with linear mixed competition with chloride.[46] In this type of competition, the binding affinity of the inhibitor (acetate) is dependent on whether the substrate (chloride) is bound. This result can be interpreted in two possible binding models: (a) one acetate binding site that changes affinity when the substrate, Cl^-, is bound, or (b), two acetate binding sites, only one of which is Cl^- dependent. Because acetate is known to bind to the nonheme Fe on the acceptor side of the OEC, as well as to a site on the donor side,[86,87] Brudvig and co-workers concluded that the linear mixed competition observed between chloride and acetate is best modeled by two acetate binding sites. To determine the effect of Cl^- on the two binding sites, they monitored the relevant EPR signals as a function of Cl^- concentration. The acceptor side binding site is characterized by the formation of the acetate-induced Fe-Q_A EPR signal; they found that the signal was formed independently of Cl^-.[46] On the other hand, both the yield of the S_2-state and the rates of formation of $S_2-Y_Z^\bullet$ and $Y_Z^\bullet$ were dependent on the concentration of both acetate and chloride. This was taken as evidence that acetate binds in competition with Cl^- on the donor side and independently of Cl^- on the acceptor side. The binding constant for chloride bound to the donor side is $K_{Cl} = 0.5 \pm 0.2$ mM; the binding constant for acetate bound to the chloride site is $K_I = 16 \pm 5$ mM.[46] Lindberg reports a similar binding constant for chloride binding at a low-affinity, rapidly exchanging site.[43] Clearly, the binding affinity for acetate is much lower than that for native chloride. It is possible that the binding is pK_a dependent.[46] For example, Sandusky and Yocum found in studies involving amine-substitution for chloride that the binding affinites for the different amines are pK_a dependent.[12] However, Wincencjusz et al. recently reported that when different anions (Br^-, I^-, NO_3^-, NO_2^-) are substituted for chloride, while the kinetics of oxygen evolution are dependent on the type of anion occupying the Cl^- site, there is no correlation to size, pK_a, or the hardness/softness of the anions studied.[19]

Because acetate and chloride compete for a donor side binding site, our ESEEM evidence showing that acetate binds at the Mn cluster, and perhaps directly to the cluster, provides strong support that chloride also binds to the cluster. This proposal has been made before, and these ESEEM results provide strong new experimental evidence. For example, Sandusky and Yocum proposed that chloride forms a bridging ligand between two manganese atoms in the cluster.[12,14] This is certainly consistent with one of the proposed acetate bridging motifs described in the ESEEM analysis (Figure 9c), though mono- and bidentate terminal ligation are also possible (vide supra; Figure 9a,b). In terms of specific S-state transitions, Wincencjusz et al.[18,19] have detected a chloride requirement for cluster oxidation in the $S_2 \rightarrow S_3$ and the $S_3 \rightarrow S_0$ transitions.[18,19] Acetate inhibits this first $S_2 \rightarrow S_3$ transition, locking the donor side in the $S_2-Y_Z^\bullet$ configuration.[48−52] As we know that acetate is bound at the S_2-state in these specifically inhibited samples, it is very likely that chloride binds to this site, proximal to manganese, in the S_2-state in oxygen evolving samples.

Acetate Competition with Other Ligands. We have examined the effect of acetate inhibition on access of methanol, DMSO, and water to binding sites in close proximity to the Mn cluster. Experiments with deuterated DMSO (Figure 7) show that this potential ligand does not bind to the Mn cluster under conditions of acetate inhibition. This was the anticipated result, given that there is no evidence for DMSO binding in control, untreated PSII samples. The ESEEM experiments with deuterated methanol (Figure 6) show no major changes in the access of methanol to the vicinity of the Mn cluster. This strongly suggests that the acetate binding site is distinct from the site or sites where methanol binds to or in close proximity to the Mn cluster. On the other hand, the ^2H modulation observed following D_2O incubation is reduced appreciably in NO/CH_3COO^--treated samples as compared to control PSII samples (Figure 8a). This effect can be examined directly by dividing the (50% D_2O/H_2O) ratioed "light minus dark" time-domain for untreated PSII by the (50% D_2O/H_2O) ratioed "light minus dark" time-domain for NO/CH_3COO^--treated PSII. This spectra is termed the "ratio of ratios" and is shown in Figure 8b. To a good approximation, this ratio reveals the modulation from deuterons displaced from the vicinity of the Mn cluster by the acetate treatment. This ^2H modulation is relatively deep. The dotted line in Figure 8b shows a simulation of the ratioed ^2H modulation using the same matrix-diagonalization ESEEM simulation program employed for the simulation of Figure 4. The simulation employs one deuteron with both isotropic and dipolar couplings ($A_{iso} = 0.800$ MHz; $A_{dip} = 0.617$ MHz), along with two deuterons with only dipolar couplings ($A_{dip} = 0.450$ MHz). A nuclear quadrupole coupling (e^2Qq) of 0.22 MHz was used for each of the three deuterons in accordance with the value used in the ESEEM study of water and methanol ligation to a mixed-valence dinuclear Mn complex.[84] The 0.617 MHz dipolar coupling of the isotropically coupled deuteron corresponds to a point-dipolar distance of 2.7 Å, while the 0.450 MHz dipolar coupling of the other two deuterons corresponds to a 3.0 Å point-dipolar distance. We note that simulations using deuterons *only* dipolar-coupled to the Mn cluster are poor because they do not exhibit enough damping in the deuteron modulation after the first few cycles. Because the samples were prepared with 50% ^2H_2O, these results indicate that approximately six exchangeable hydrogen atoms in the immediate vicinity of the Mn cluster are displaced by acetate binding, two of which have appreciable isotropic hyperfine coupling to the Mn cluster.[88] The short distances (in the point-dipolar approximation) and the displacement of two deuterons with appreciable isotropic couplings suggest that acetate displaces at least one S_2-state water ligand to the cluster. If this water displacement disrupts any coupling between proton and electron transfer necessary to reduce $Y_Z^\bullet$ in the $S_2 \rightarrow S_3$ transition, this could explain why acetate blocks the OEC from advancing past the $S_2-Y_Z^\bullet$ state. We also note the possibility that the acetate treatment could

(86) Deligiannakis, Y.; Petrouleas, V.; Diner, B. A. *Biochim. Biophys. Acta* **1994**, *1188*, 260−270.
(87) Petrouleas, V.; Deligiannakis, Y.; Diner, B. A. *Biochim. Biophys. Acta* **1994**, *1188*, 271−277.

(88) Because the ESEEM modulation is a product of *each* nuclear contribution,[60] the ESEEM modulation observed in PSII membranes treated with 100% D_2O should correspond to the *square* of the modulation observed in PSII membranes treated with 50% D_2O.

$$V_{mod}(100\%D_2O) = V_{mod}(50\%D_2O)^*V_{mod}(50\%D_2O) \qquad (8)$$

Indeed, this is observed experimentally (unpublished data). Thus, we can scale the simulation presented in Figure 8b to reflect the case of a PSII sample prepared with 100% D_2O. We find that in fully deuterated water, acetate displaces two deuterons with both isotropic ($A_{iso} = 0.800$ MHz) and dipolar ($A_{dip} = 0.617$ MHz) couplings and four deuterons with only dipolar couplings ($A_{dip} = 0.450$ MHz).

displace both a water and a chloride ligand if acetate binds as a bidentate or bridging ligand.

Acknowledgment. We most gratefully acknowledge the National Science Foundation (MCB 9513648) and the National Institutes of Health (GM48242) for supporting this work. We would like to thank Dr. Jeff Peloquin for his help creating the "dangler" model contour plot.

JA012036C